

Linear and nonlinear time series analysis of the black hole candidate Cygnus X-1

Jens Timmer¹, Udo Schwarz², Henning U. Voss², Ingo Wardinski², Tomaso Belloni³, Günther Hasinger⁴, Michael van der Klis³, and Jürgen Kurths^{2*}

¹ *Zentrum für Datenanalyse und Modellbildung, Universität Freiburg, Eckerstr. 1, D-79104 Freiburg, Germany*

² *Institut für Physik, Universität Potsdam, D-14469 Potsdam, Potsdam, Germany*

³ *Astronomical Institute “Anton Pannekoek”, University of Amsterdam, Kruislaan 403, NL-1098 SJ Amsterdam, The Netherlands*

⁴ *Astrophysikalisches Institut Potsdam, An der Sternwarte 16, D-14482 Potsdam, Germany*

(October 1, 2018)

We analyze the variability in the X-ray lightcurves of the black hole candidate Cygnus X-1 by linear and nonlinear time series analysis methods. While a linear model describes the over-all second order properties of the observed data well, surrogate data analysis reveals a significant deviation from linearity. We discuss the relation between shot noise models usually applied to analyze these data and linear stochastic autoregressive models. We debate statistical and interpretational issues of surrogate data testing for the present context. Finally, we suggest a combination of tools from linear and nonlinear time series analysis methods as a procedure to test the predictions of astrophysical models on observed data.

PACS: 05.40.+j, 02.50.Wp, 97.80.Jp

I. INTRODUCTION

Cygnus X-1 is one of the best established black hole candidates. Mass accretion from its primary HDE 226868 leads to X-ray emission which exhibits a variability on time scales of tenths of seconds [1] up to months [2]. The shorttime variability is assumed to be caused by instabilities of the accretion disk and is usually formally described by shot noise models [3–5] which are a specific kind of point processes. These models are inspired by hypotheses about the physics of the accretion process and the processing of X-rays by Comptonization in the neighborhood of the black hole. Free parameters of these models, like morphology and distribution of the shots, are usually tuned to fit the observed energy or power spectra.

On the other hand, starting from the observed data and characterizing the dynamical structure of this observed variability by time series analysis methods might yield valuable constraints on astrophysical models. This characterization can be, for example, a fit of an explicit model to the data or the extraction of a feature which captures some typical structure of the dynamics. Such a characterization could either inspire new astrophysical

models or could be used for additional tests of the predictions of existing models. Of course, there is no direct way for a characterization neither by modeling nor by feature extraction of observed data to an astrophysical model: On the one hand, although the goodness-of-fit of a diagnostic model can be evaluated by statistical tests, these tests might have low diagnostic power to detect a misspecification of the model. On the other hand, a certain feature discovered in the data might be generated by many different types of dynamics. Therefore, before drawing conclusions about the underlying process from data analysis, different independent approaches should be used and the plausibility of a fitted model or an extracted feature should be judged in the light of astrophysical knowledge.

The first step of nonlinear time series analysis is usually to study the structure of a possible underlying attractor. However, methods from nonlinear dynamics did not succeed to establish a low-dimensional attractor for X-ray lightcurves of Cygnus X-1 [6]. It is also important to mention that time series analysis methods usually assume that the underlying process presents a dynamical system in contrast to a shot noise model.

As an alternative to the commonly applied shot noise models, the linear state space model (LSSM) as a generalization of dynamical linear autoregressive models including the observational noise has been proposed to model the X-ray variability of active galactic nuclei in [7]. Two attractive properties of this approach are, firstly, that the LSSM can be fitted to the data in the time domain and, secondly, that it explicitly takes the observational noise covering the dynamics into account. The state space model has been applied to data from Cygnus X-1 in its low state [8]. This analysis has revealed that a first order autoregressive process describes the dynamics of the X-ray variability well. This predicts a shot noise model with an exponential decay and a very specific mode of excitation of these shots.

In this contribution, we analyze X-ray lightcurves of Cygnus X-1 from its low and intermediate state by the LSSM as well as by a method which is able to capture deviations from linearity. In accordance with [8], a scalar LSSM results in a fit that explains the linear correlations of the time series well. However, the nonlinear analy-

*Juergen@agnld.Uni-Potsdam.de

sis using a measure for time reversibility of the process, reveals strong deviations from linearity on exactly that dynamical time-scale found by the LSSM. To interpret this result consistently, we discuss the mathematical and astrophysical implications of linear stochastic and shot noise models.

Finally, we suggest a combination of tools from linear and nonlinear time series analysis methods as a procedure to test the predictions of astrophysical models on observed data.

The organization of the paper is as follows: In Section II we introduce the data under investigation. In Section III we discuss shot noise and linear stochastic models and their relation. Furthermore, we explain how we use the method of surrogate data to test for time reversibility. Section IV presents the results, which are discussed in Section V.

II. THE DATA

The data were recorded with the Proportional Counter Array (PCA) on board the Rossi X-ray Timing Explorer (RXTE). The X-ray activity of Cygnus X-1 is classified as low, intermediate, and high, depending on the mean count rate [9]. Our analysis is based on two data sets: The first data set was recorded on 22nd May 1996, 19:05:12 - 19:48:02, while Cygnus X-1 was in its intermediate state [9]. The energy range was 2.0 - 14.1 keV (channel range: 0-35). The sampling frequency was 256 Hz and the data set consists of 655,360 data points. The mean number of counts per bin was 38.3 with standard deviation 10.0. The second data set was recorded on 12th February 1996, 9:37:20 - 10:03:06, while Cygnus X-1 was in its low state. The energy range was 2.0 - 9.9 keV (channel range: 0-35). The sampling frequency was 256 Hz and the data set consists of 394,752 data points. The mean number of counts per bin was 18.7 with standard deviation 7.1. Figure 1 displays a 3 s segment of the first data set. A part of the variability of the data is explained by the fact that the recording process is a counting process. This leads to additive uncorrelated observational noise which is Poisson distributed. Due to the high mean count rate this Poisson noise is well approximated by Gaussian noise.

III. METHODS

A. Shot noise processes

Shot noise processes are a specific type of point processes [10]. Point processes are characterized by a probabilistic law that some event happens at a certain time. For the simplest form of a shot noise model the probabilistic law of occurrence of events follows a Poisson process and the event is an exponential decay with initial

value M and decay time τ . A Poisson process is defined by the property that the probability of an event to take place in a time interval $(t, t + \Delta t)$ is proportional to Δt in the limit of small intervals:

$$\lim_{\Delta t \rightarrow 0} \text{prob}(\text{Event in}(t, t + \Delta t)) = \rho \Delta t, \quad (1)$$

where ρ denotes the intensity of the process. The sampled time series consists of a superposition of the single shots at times T_j whose occurrence follows Eq. (1), i.e.,

$$x(t_i) = \sum_j M \Theta(t_i - T_j) e^{-(t_i - T_j)/\tau} \quad (2)$$

with $\Theta(z) = 1$ if $z \geq 0$, $\Theta(z) = 0$ if $z < 0$. We call this process the classical shot noise process.

The power spectrum of this process (2) is given by [11]:

$$S(\omega) = \frac{M^2 \rho}{1/\tau^2 + \omega^2}, \quad \omega \neq 0. \quad (3)$$

The classical shot noise has already been proposed in Ref. [3] to describe the observed variability of the lightcurves of Cygnus X-1. It consists of exponentially decaying shots with fixed initial value which occur in time with a constant rate of probability. Several generalizations have been proposed: Shots with a decay rate drawn from a certain distribution have been suggested in [4,12,13]. A distribution for the initial values of the shots was considered in [14]. Vikhlinin et al. [15] introduced interactions between different shots. Furthermore, the simple exponential form was replaced by more complicated time courses showing an initial increase from zero to a maximum value followed by a decay to zero [8]. These types of profiles are supported by Monte Carlo simulations of astrophysical models of the X-ray processing by spatially resolved Comptonization in a cloud of hot electrons surrounding the accretion disk [16].

For some generalized shot noise models the power spectra can be calculated analytically [5,11]; otherwise they have to be estimated from simulated data.

B. Linear stochastic dynamical systems

In contrast to shot noise processes given by Eqs. (1,2), continuous dynamical systems are given by a differential equation

$$\dot{\vec{x}} = \vec{f}(\vec{x}, \vec{\epsilon}), \quad (4)$$

where $\vec{\epsilon}$ denotes random perturbations which might influence the time evolution of the dynamics. An attractive feature of modeling time series by dynamical systems is that the specific form of $\vec{f}(\vec{x}, \vec{\epsilon})$ might provide insight in the physics at work, see [17,18] for two examples from physics and [19,20] for application to physiological time series.

In the simplest case if $f(\cdot)$ is linear in \vec{x} and the dynamical noise $\vec{\epsilon}$ is Gaussian distributed and additive, the system represents linear combinations of damped oscillators and relaxators that are driven by Gaussian noise. Since the model is linear, all information about the model is captured by the power spectrum. For a scalar dynamics:

$$\dot{x} = -\alpha x + \epsilon, \quad \epsilon \sim WN(0, \sigma^2), \quad (5)$$

the spectrum is given by:

$$S(\omega) = \frac{\sigma^2}{\alpha^2 + \omega^2}. \quad (6)$$

It is important to emphasize that first order linear stochastic dynamical systems have the same ω -dependence of the spectrum as the classical shot noise model, see Eq. (3).

Most often, \vec{x} cannot be observed directly, but only a scalar function $g(\vec{x})$. Furthermore, the observation y might contain additive measurement noise, denoted by η :

$$y = g(\vec{x}) + \eta. \quad (7)$$

While the noise $\vec{\epsilon}$ in Eq. (4) drives the dynamics, the measurement noise η in Eq. (7) only disturbs the observation of the system. For the case of a linear dynamical system, Eq. (5), with white additive observational noise of variance R , the spectrum reads:

$$S(\omega) = \frac{\sigma^2}{\alpha^2 + \omega^2} + R. \quad (8)$$

Since measured data are sampled, discrete time dynamical models

$$\vec{x}(t) = \vec{h}(\vec{x}(t - \Delta t), \vec{\epsilon}(t)), \quad (9)$$

are often used. If both the dynamical and the measurement noise are Gaussian distributed, and the functions \vec{h} and g are linear, i.e.,

$$\begin{aligned} \vec{x}(t) &= A\vec{x}(t - \Delta t) + \vec{\epsilon}(t), & \vec{\epsilon}(t) &\sim N(0, Q), \\ y(t) &= C\vec{x}(t) + \eta(t), & \eta(t) &\sim N(0, R), \end{aligned} \quad (10)$$

the linear state space model (LSSM) as a generalization of the well known autoregressive (AR) models results. They represent discrete time versions of the continuous time linear stochastic models. The matrix A determines the dynamics of the unobserved state vector $\vec{x}(t)$. Its dimension reflects the order of the process. The vector C maps the state vector to the observation. In the case of a scalar dynamics, A is related to the relaxation time scale τ by $\tau = -1/\log|A|$. The mathematical formalism of the LSSM and procedures to estimate its parameters are described in detail in [19,21].

To test the consistency of a fitted model with the data, at least three criteria should be applied.

1. The variance of the prediction residuals does not decrease significantly for larger model dimensions.
2. The spectra calculated from the fitted LSSM for larger model dimensions coincide.
3. An appropriate model should turn the correlations in the data into prediction residuals consistent with white noise. In the frequency domain this hypothesis can be tested by comparing the periodogram of the residuals with the expected straight line in the case of white noise by the Kolmogorov-Smirnov test [22].

C. Noise reduction

Measured time series of natural systems often contain a large amount of additive observational noise. The fitted LSSM can be applied as a linear filter to perform a noise reduction on the data even if it is misspecified as a dynamical model of the underlying process. If the LSSM describes the second order properties of the process correctly, the LSSM is the optimal linear filter [21].

Algorithmically the noise reduction is achieved by first applying the Kalman filter, which yields an estimate of $\vec{x}(t)$ based on the observed data $y(1), y(2), \dots, y(t)$. Then the so-called smoothing filter is applied backwards in time to obtain estimates $\hat{\vec{x}}(t)$ based on the whole data set [21]. The possibility to apply this smoothing filter relies on the property of linear stochastic processes to be time reversible, see Section III D. Multiplication of $\vec{x}(t)$ by the estimated C yields an estimate of the noise-free scalar observable $y(t)$.

The statistical properties of the estimated $\hat{y}(t)$ can be understood in the frame of Bayesian estimation, see [23] for a detailed discussion. The model with its fitted parameters represents a prior on the smoothness of the hidden $\vec{x}(t)$. Conditioned on this prior a maximum likelihood estimate of $y(t)$ is obtained. The estimated time series is the most probable one assuming the validity of the model, Eq. (10).

It should be emphasized that the estimated time series does not represent a typical realization of the fitted model used as prior. Even if the fitted model is the true one, the estimated time course is a slightly low-pass filtered version of a typical realization. If the fitted model is, however, not the true model, the estimated time series will show statistical properties which, literally spoken, lie between those of the process which generated the data and the model used as prior. Especially, if the true process is nonlinear showing a strong time irreversibility, this quantity might be reduced for the estimated time series. Thus, the procedure does not lead to false positive results.

D. The relation between linear models and shot noise models

Linear autoregressive and shot noise processes are both stochastic processes. The randomness driving these processes usually reflects the restricted knowledge about the dynamics at work. Often, the dynamics is exposed to numerous influences that cannot be taken into account explicitly. Even if these influences are deterministic in nature they effectively act as random influences due to their large number. The characteristic difference between autoregressive and shot noise processes is the way the randomness enters the process: i) In dynamical processes it describes a random force that influences the dynamics in every instant of time. ii) In point processes it acts as a trigger that generates a certain event only at certain points in time.

However, there is a formal connection between the classical shot noise process and the scalar linear stochastic dynamical process. Formally, and “not in the spirit of point processes” [10], one can transform Eq. (2) into

$$x(t) = (1 - \Delta t/\tau) x(t - \Delta t) + \epsilon(t), \quad (11)$$

where $\epsilon(t)$ has the specific form:

$$\epsilon(t) = \begin{cases} 0 & \text{with probability } 1 - \rho\Delta t \\ M & \text{with probability } \rho\Delta t \end{cases}. \quad (12)$$

Thus, for $\rho\Delta t \approx 1$ and M following a Gaussian distribution, there is a formal equivalence between the scalar linear autoregressive process and the classical shot noise process which is characterized by its exponentially decaying shot profile. In practice Δt corresponds to the sampling interval. The condition $\rho\Delta t \approx 1$ means that the process is highly undersampled, since single shots are not resolved. The required Gaussianity of the distribution of the initial values of the shots does not meet the physical constraint of positivity in the astrophysical context of X-ray bursts. In the limit $\rho\Delta t \approx 1$ it might be an effective description resulting from the superposition of the unresolved Poisson process.

In summary, scalar linear dynamical processes are a certain formal limiting case of shot noise models. Only in the case of linearity, there is no interaction between the excitations and time course of the shots. It should be noted that, in general, nonlinear stochastic dynamical systems cannot be formulated as a formal limit of shot noise models.

E. Beyond linear models: Time irreversibility

An important property of linear Gaussian processes is time reversibility, i.e., the statistical properties of the process are the same forward and backward in time [24]. An intuitive explanation is that the statistical properties of these processes are completely captured by the

autocorrelation function, which is by definition symmetric under time reversal. Shot noise processes with non-symmetric shot profiles are not time reversible as are many nonlinear dynamical systems. The Gaussianity of the noise $\epsilon(t)$ of a linear autoregressive process is crucial for the time reversibility. Any deviation from Gaussianity leads to time irreversibility even in the case of linear dynamics [24]. This is of special interest in view of Eq. (12). While time reversibility has been used to test for nonlinearity in dynamical systems, [25–28], we will use it here as an indicator for a shot noise model. A test for time irreversibility in this context will be discussed in the next section.

F. Nonlinear analysis: The method of surrogate data

The theory of nonlinear dynamical systems offers notions to characterize processes beyond linearity, see [29,30] for a review. Different quantities have been invented to reveal whether an observed time series is a realization of a chaotic system; among others, the correlation dimension [31], Lyapunov exponents [32], and nonlinear forecasting errors [33]. It has been observed later that due to the finite size of data, noise, and linear correlations, the algorithms to calculate these quantities can give false positive results.

To test the reliability of the results, the method of surrogate data has been invented independently by different authors, e.g. [34–38], but has been made most popular by [25]. It has found wide applications in the analysis of astrophysical [36,39–41], geophysical [42–44] and biophysical [45–47] data.

The general idea is to simulate time series whose statistical properties are constrained to the null hypothesis one wants to test for [48]. In testing for linearity this is achieved by randomizing the phases of the Fourier transform of the data and transforming the result back to the time domain. A possible static nonlinearity in the observation, $g(\vec{x})$ in Eq. (7), is known to produce spurious significant results [49]. Therefore, a proper adjustment of the distribution of the time series data is performed. For many realizations of time series from this procedure, the same algorithm as to the original data is applied leading to a distribution of the feature calculated by the algorithm assuming linearity. A significant difference between the distribution of the feature produced by the algorithm for the surrogate data and the original data is taken as an indication that the process underlying the original is not a Gaussian, stationary, stochastic, linear one. A significant result of the test does not necessarily indicate chaoticity of the process, since this is only one possibility to violate the null hypothesis.

Former analysis revealed that it is unlikely that the Cygnus X-1 as well as other comparable X-ray sources represent a low-dimensional chaotic system [6,50,51]. Therefore, we apply the surrogate data test to look for

deviations from the null hypothesis in general.

The results of the surrogate data test for a feature f are usually reported as significance S :

$$S = \frac{|f - \langle f \rangle_{surr}|}{\sigma_{surr}}, \quad (13)$$

where $\langle f \rangle_{surr}$ denotes the mean of the distribution of the feature for the surrogates and σ_{surr} its standard deviation. Assuming a Gaussian distribution for the feature a value of $S = 2.6$ corresponds to a significance level of $\alpha = 0.01$.

We propose here a surrogate data analysis based on time reversibility. Generalizing a suggestion of Weiss [24], a simple measure denoted by $Q(m)$ for a deviation from reversibility for a certain time lag m was introduced in [25]:

$$Q(m) = \frac{\langle (x(t+m) - x(t))^3 \rangle}{\langle (x(t+m) - x(t))^2 \rangle}. \quad (14)$$

More complex measures for time irreversibility based on conditional, respectively joint probability distributions are described in [26–28].

Since it is not clear beforehand at which lag m a possible deviation from the null hypothesis might result in a significant $Q(m)$ statistics, the significances $S(m)$ will be evaluated for all lags up to a maximum lag. This leads to the statistical problem of multiple testing. It is important to emphasize that this has an impact on the level of significance α , i.e., the probability to reject the null hypothesis although it is true. If the null hypothesis is tested in n independent tests at the level α , the probability to reject the null hypothesis at least once is given by

$$\tilde{\alpha} = 1 - (1 - \alpha)^n. \quad (15)$$

For example, for $\alpha = 0.01$ and $n = 10$, the actual significance level $\tilde{\alpha}$ is 0.1, leading to a ten times higher probability for an incorrect rejection of the null hypothesis than expected. A simple cure to this problem is the Bonferroni-correction [52]. Therefore, Eq. (15) is solved for α :

$$\alpha = 1 - (1 - \tilde{\alpha})^{1/n}. \quad (16)$$

Since $\tilde{\alpha} \ll 1$, the right hand side of Eq. (16) can be approximated in first order, resulting in the simple rule:

$$\alpha = \tilde{\alpha}/n. \quad (17)$$

This procedure is known to be extremely conservative, i.e., while it guarantees that the significance level is correct, the test loses its diagnostic power to detect a violation of the null hypothesis. For some test statistics, procedures are known to obtain tests that have the correct significance level as well as a good diagnostic power, see e.g. [52–54]. It is not known to the authors, how to

apply an analogous strategy to the $Q(m)$ statistics. The main problem is that the correlations in the time series produced by the underlying dynamics of the process lead to correlations between the $Q(m)$ statistics for different lags. Thus, the only cure known to the authors is to check whether the results of an analysis of one time series can be reproduced by the analysis of independent measurements. Therefore, we subdivide our time series into segments of length 20,000 data points each and calculate the averaged $Q(m)$ statistics and its confidence interval.

To reveal the expected behavior of the $Q(m)$ statistics for shot noise processes, we simulate an exponential shot noise process with intensity $\rho = 0.1$, $\tau = 15$, initial values M_i drawn from a uniform distribution in the interval $[0,1]$, and apply the $Q(m)$ statistics. Figure 2a shows a segment of the simulated data. Figure 2b and c display the $Q(m)$ statistics and the significances $S(m)$ for different lags m based on a realization of the process of length 20,000 data points. The monotonically decaying behavior of the $S(m)$ curve does not depend on the intensity, the relaxation time or the distribution of the shot noise process. Of course, the quantitative behavior does. Classical shot noise and first order linear stochastic dynamical systems can not be discriminated by linear methods since their spectra coincide. The simulation shows that higher order statistical properties allow for a discrimination. Next we apply this concept to the analysis of measured data.

IV. RESULTS

We discuss the results for the time series of the intermediate state in detail. For the linear analysis, the results for the intermediate and low state data are comparable. Differences for the nonlinear analysis will be presented in more detail in Section IV B.

A. Linear analysis by state space models

We fit linear state space models (LSSM), Eq. (10), of increasing dimension to segments of the intermediate state time series of length 20,000. In accordance with the results of [8] for the low state, the residual variance is constant for all models of dimension larger than zero. Furthermore, the analysis reveals an equal contribution of signal and noise to the total variance of the time series.

Figure 3 displays the periodogram of the first segment and the spectra calculated from fitted one- to three-dimensional models on a log-linear and on a log-log scale. The spectrum calculated from the fitted parameters well explains the over-all periodogram of the data. Furthermore, there is no significant difference between the spectra of fitted different dimensional processes. The relaxation time of the scalar model is 14.2 sampling units cor-

responding to 55 ms. The Kolmogorov-Smirnov test does not reject the hypothesis of white noise residuals at the 1% level of confidence.

With respect to the dimension of the model, a fit of LSSMs of dimension one to three to the remaining 31 segments confirms the result for the first segment. For the pieces of 20,000 data points as well as for the whole data set the spectra calculated from the estimated parameters do not differ from the spectra of the scalar model. The estimated relaxation times range from 12.4 to 17.4 sampling units, corresponding to 48 to 68 ms. For the data set from low state the qualitative results of the linear analysis are the same as for the intermediate state, but the relaxation times range from 40 to 56 sampling units, corresponding to 150 to 220 ms, in accordance with the results reported in Ref. [8].

Linear analysis methods, like spectral analysis, only capture the second order statistical properties of a process. For linear processes the higher order properties are a function of the second order correlations. This does not hold for nonlinear processes. Therefore, it could be possible, that there is some nonlinear dynamics at work in the process under investigation which is invisible for a linear analysis. If such nonlinear dynamics can be described by Eq. (4), it can be concluded that its dimension is not larger than one. Any higher dimensional continuous-time system would have led to a difference between the spectra of the one and the higher dimensional LSSMs, since it would produce linear correlations for an order of at least the dimension of the process. In the same line of argument, a nonlinear first order dynamical process should have effected the higher order spectra. Thus, the linear analysis strongly suggests a linear stochastic first order process for a description of the data in the frame of dynamical systems.

B. Nonlinear analysis

First, we apply the surrogate data based search for deviations from linearity as described in Section III F to segments of length 20,000 up to a maximum lag of 1000 sampling units corresponding to 3.9 s of the observation. We use 100 surrogate data sets to estimate the mean and the variance of the $Q(m)$ statistics, Eq. (14) for the null hypothesis of linearity to calculate the significances $S(m)$, Eq. (13).

For the first segment, at above lag 800 the significance $S(m)$ of the $Q(m)$ statistics for time reversibility results in a value larger than 4 (Figure 4a). This corresponds to a probability for the null hypothesis smaller than 10^{-4} . As discussed in Section III F, the results of the nonlinear analysis by the surrogate data method using the $Q(m)$ statistics has to be based on the consistency of the results for independent measurements due to the multiple testing problem. Figures 4b–d display the results for the following 20,000 data point segments of the time series.

There is no consistent deviation from the null hypothesis for any lag.

Linear analysis reveals that the signal to noise ratio is equal to one if measured in relative amplitudes. This large amount of observational noise diminishes the diagnostic power of the surrogate data test to detect a possible time irreversibility. As discussed in Section III B, the LSSM can be applied to estimate the noise-free dynamical time series within a Bayesian framework. Figure 5 displays the results for the Kalman (and smoothing)-filtered data based on the one-dimensional LSSM analogous to Fig. 4. For large lags no significant changes appear apart from a smoother behavior of the curve which results from the low-pass filter property of the estimation procedure as discussed on Section III B. But for small lags the behavior of the curves changes: Figure 6 shows the significances $S(m)$ of the $Q(m)$ statistics for the first 100 lags. Consistently, a significant deviation from linearity is found for exactly those lags up to the time scale of approximately 15 sampling units that was found as typical time scale by the linear analysis. Note that the resulting $S(m)$ curves for the Kalman-filtered data resemble the decaying curve expected for a shot noise model, Fig. 2, while the raw data suggest a maximum at around 10 sampling units. The similarity of the results for larger time scales and the differences for short time scales can be interpreted in the frame of shot noise models. For lags much larger than the relaxation time of the shots, the data are independent and the $Q(m)$ statistics is expected to vanish. The appearance of the $S(m)$ is determined by correlated fluctuations, as discussed in Section III F. For time scales smaller than the relaxation time of the shots, the $Q(m)$ statistics is significantly different from zero, see Fig. 2. The difference between the results for the raw and the Kalman-filtered data is an effect of the lag dependent signal to noise ratio. This is most pronounced for the shortest lags, since the time-course of each shot is continuous, but the observational noise is discontinuous, leading to a decreasing signal to noise ratio for smaller lags. This is the reason why $S(m)$ tends to zero for lags close to zero for the raw data.

Since the Kalman filter is linear, it is not expected to lead to artificial results. This has been confirmed in a simulation study. We use the fitted one-dimensional LSSM to generate data and calculated the significance $S(m)$ of the $Q(m)$ statistics for these data and data obtained by the Kalman filter. The results are displayed in Fig. 7 and show that the Kalman filter does not produce spurious results for processes that are time reversible. Simulation studies using shot noise processes with added observational noise show that the Kalman-filtered data reproduce the behavior of the $S(m)$ curve for shot noise processes as displayed in the Fig. 2. Thus, the significant results are not due to the Bayesian estimation by the Kalman filter (Section III B). This is reasonable since in the worst case this linear filtering “pulls” the data in the direction of behaving more linear. That means that an existing time irreversibility would be decreased, but no

spurious significant effects are introduced.

Figure 8 shows the mean and 2σ confidence region of the significance $S(m)$ of the $Q(m)$ statistics obtained from the 32 segments of length 20,000 based on the raw and the noise-reduced time series from the intermediate state. Figure 9 displays the corresponding plot for the 19 segments from the low state time series. For both data sets the $S(m)$ curves for the raw and the Kalman-filtered time series are statistically indistinguishable for larger lags. Significant differences arise only for small lags. Based on the analysis of the raw data, any kind of shot noise model would be rejected. For the analysis based on the Kalman-filtered data, the $S(m)$ curve for the low state time series suggests a classical shot noise model by its decay for small lags and insignificant values for larger lags, compare Fig. 2. For the intermediate state time series, a significant maximum occurs at a lag m of 30 sampling units, corresponding to 117 ms. This maximum cannot be reproduced by a simple shot noise model and calls for more complex processes discussed in Section III A.

For both time series, our analysis shows that the linear state space model is not an appropriate model to describe the data, since the significant time reversibilities calculated based on the fitted models contradict the assumption of these models. It is, however, important to note that the LSSM can be used to perform an efficient noise reduction.

V. DISCUSSION

We have developed methods and have discussed how it is possible to decide based on measured data whether a time series that even comprises a large amount of additive observational noise has been produced by a scalar linear stochastic dynamical system or a shot noise process. We have shown that linear spectral analysis does not allow for a discrimination. The nonlinear property of time irreversibility of shot noise processes form the basis for a significant distinction. A straightforward evaluation of this feature is hampered by the statistical problem of multiple testing and effects of additive observational noise. We have discussed how these problems can be overcome.

We have applied methods from linear and nonlinear time series analysis to two X-ray variability lightcurves of the black hole candidate Cygnus X-1. The first time series was recorded while Cygnus X-1 was in an intermediate state [9], the second represents the low state. Such data are usually described by shot noise models, a specific kind of point processes. Although point processes are fundamentally different from dynamical systems, they share some properties with the latter. First, the spectrum of the classical shot noise process coincides with that of a scalar continuous time linear Gaussian stochastic process. Second, most shot noise models share the property of most nonlinear dynamical systems of be-

ing time irreversible.

Firstly, we have fitted linear state space models (LSSM) of increasing dimension to segments of the data. The variance of the prediction residuals is not decreasing for models of dimension larger than zero and the spectra calculated from the fitted parameters of the different models coincide, suggesting a scalar dynamical model. Testing the consistency of the prediction residuals with white noise has revealed a good over-all fit. The linear analysis shows that if the process is a dynamical system, it is linear and one-dimensional. Any higher dimensional or continuous-time nonlinear dynamical systems would have led to differences between one and higher dimensional LSSMs with respect to the spectra calculated from the fitted parameters and the variance of the prediction residuals. Furthermore, the analysis suggests a signal to noise ratio of one.

Fitting a LSSM to data in the time domain is asymptotically equivalent to fitting its spectrum to the periodogram of the data in the frequency domain [55]. The spectrum of the classical shot noise process is identical with the spectrum of a first order linear dynamical process. Thus, even if a goodness-of-fit test in the frequency domain does not reject a LSSM, no discriminating conclusions can be drawn with respect to the question whether a dynamical system or a shot noise process has generated the data. Therefore, astrophysical interpretations of the parameters of fitted LSSMs [8,56,57] should be treated with care.

Astrophysical studies indicate that the processes under investigation follow some kind of shot noise model [3–5,8,13,16,58–60]. In general, shot noise models are not reversible in time. Surrogate data testing for time irreversibility for different lags introduces the multiple testing problem. Therefore, we have investigated whether consistent results could be obtained from an analysis of segments of the time series.

For the raw data of the low state time series, no significant deviation from linearity has been detected. However, we have found a double well behavior of the $Q(m)$ statistics in the case of the intermediate state data (Fig. 8). Both results contradict a simple shot noise model. This might have been caused by the low signal to noise ratio. In the frame of Bayesian estimation based on a fitted LSSM, we have applied the Kalman filter to get a noise-reduced time series. Based on these noise-reduced data, we have found a significant deviation from linearity at that time scale found by linear analysis that are in accordance with results for simulated data from a simple shot noise model. While the results for the low state time series are in agreement with a simple shot noise model with independently decaying shots, the intermediate state time series shows a more complex behavior. Apart from the decay for small lags the significances show an additional distinct maximum. Our results are based on the estimated noise-reduced time series obtained by the LSSM. Any noise reduction procedure imposes assumptions about the underlying process

and might lead to artifacts if the assumptions are not met as in the present study. In the case considered here a violation of the assumptions of the model, in the worst case, leads to less significant results since the filter is linear. Thus, the procedure is statistically conservative even if the model is misspecified.

By its qualitative difference to the results for simple shot noise models for the intermediate state time series, the $Q(m)$ statistics as a measure for time irreversibility poses a constraint on astrophysical models for this phenomenon. It has been shown that the classical shot noise model (1–3) does not satisfactorily describe the process under consideration [9]. Therefore, one has to search for more complex models. For such models the significance of the $Q(m)$ statistics (Fig. 8) provides an additional and independent test beyond the usually applied energy and power spectra. For example, our results exclude shot noise models with symmetrical rise and decay of the shots as discussed in [58], since such models would not lead to a violation of time reversibility. In general, one has to Kalman-filter the data generated by the proposed model in the same way as the observed data and test the compatibility of the resulting $S(m)$ curve statistically.

No explicit test to decide whether a dynamical system or a shot noise process underlies a measured time series is known to the authors. Summarizing the results from the linear and the nonlinear time series methods, the analysis strongly suggests that a shot noise model is at work. This is in accordance with astrophysical considerations: X-rays undergo multiple Compton scattering in the corona of hot electrons surrounding Cygnus X-1. The shots represent the projection of this spatio-temporal, reaction-diffusion like processes on the time axis. The loss of spatial resolution causes that the resulting process cannot be formulated as a dynamical system anymore. This reveals an interesting aspect of surrogate data testing that might also apply for other applications [41]. Initially, testing by surrogates was introduced to support the detection of chaotic dynamics. Later, it was recognized that a rejection of the null hypothesis of linear, stochastic, stationary, Gaussian dynamics does not necessarily indicate chaos, i.e., a special type of nonlinear, stationary, deterministic dynamics, since there are other possibilities to violate the assumptions of the above null hypothesis [61–64]. Furthermore, surrogate data testing was characterized as not too informative if simple inspection of the data reveals a deviation from the null hypothesis [61]. In the present case, the linear analysis looks promising at first sight rendering the surrogate data test informative. But here, the reason for a significant surrogate data test is not chaotic nonlinearity, but the projection from the spatio-temporal into the temporal domain. Thus, the X-ray variability data offer a new possibility for a rejection of the null hypothesis of a linear dynamical system: The system is not a dynamical system of the form $\dot{\vec{x}} = \vec{f}(\vec{x}, \vec{\epsilon})$ at all.

In summary, following a quotation of G.E.P. Box: “All

models are wrong, but some are useful”, we propose the use of the misspecified linear state space model together with the measure of time reversibility inspired by nonlinear dynamics as an additional test to the usually applied energy and power spectra to evaluate the validity of astrophysical shot noise models on measured data.

VI. ACKNOWLEDGMENTS

The authors acknowledge the stimulating atmosphere of the Isaac Newton Institute where parts of this article were written. J.T. acknowledges the hospitality of the University of Potsdam. H.U.V. acknowledges financial support by the Max-Planck-Gesellschaft.

-
- [1] M. Oda, P. Gorenstein, and H. Gursky, *Astrophys. J.* **166**, L1 (1971).
 - [2] J. C. Kemp *et al.*, *Astrophys. J.* **271**, L65 (1983).
 - [3] J. Terrell, *Astrophys. J.* **174**, L35 (1972).
 - [4] T. Belloni and G. Hasinger, *Astron. Astrophys.* **227**, L33 (1990).
 - [5] J. Lochner, J. Swank, and A. Szymkowiak, *Astrophys. J.* **376**, 295 (1991).
 - [6] J. Lochner, J. Swank, and A. Szymkowiak, *Astrophys. J.* **337**, 823 (1989).
 - [7] M. König and J. Timmer, *Astron. Astrophys.* **124**, 589 (1997).
 - [8] K. Pottschmidt, M. König, J. Wilms, and R. Staubert, *Astron. Astrophys.* **334**, 201 (1998).
 - [9] T. Belloni *et al.*, *Astrophys. J.* **472**, L107 (1996).
 - [10] D. Cox and V. Isham, *Point Processes* (Chapman and Hall, London, 1980).
 - [11] A. Papoulis, *Probability, random variables and stochastic processes* (McGraw–Hill, New York, 1984).
 - [12] P. Nolan *et al.*, *Astrophys. J.* **246**, 494 (1981).
 - [13] S. Miyamoto and S. Kitamoto, *Nature* **342**, 773 (1989).
 - [14] H. Lehto, in *Proc. 23rd ESLAB Symp. X-ray Astronomy*, edited by J. Hunt and B. Battrick (ESA, Noordwijk, 1989), p. 499.
 - [15] A. Vikhlinin, E. Churazov, and M. Gilfanov, *Astron. Astrophys.* **287**, 73 (1994).
 - [16] J. Dove, J. Wilms, M. Maisack, and M. Begelman, *Astrophys. J.* **487**, 759 (1997).
 - [17] H. Voss, A. Schwache, J. Kurths, and F. Mitschke, *Phys. Lett. A* **256**, 47 (1999).
 - [18] R. Hegger, H. Kantz, and F. Schmöser, *CHAOS* **8**, 727 (1998).
 - [19] J. Timmer, *Int. J. Bif. Chaos* **8**, 1501 (1998).
 - [20] S. Michalek *et al.*, *Euro. Biophys. J.* **28**, 605 (1999).
 - [21] J. Honerkamp, *Stochastic Dynamical Systems* (VCH, New York, 1993).
 - [22] W. Press, B. Flannery, S. Saul, and W. Vetterling, *Nu-*

- merical Recipes in C* (Cambridge University Press, Cambridge, 1992).
- [23] G. Kitagawa and W. Gersch, *Smoothness priors analysis of time series*, No. 116 in *Lecture Notes on Statistics* (Springer, New York, 1996).
- [24] G. Weiss, *J. Appl. Prob.* **12**, 831 (1975).
- [25] J. Theiler *et al.*, *Physica D* **58**, 77 (1992).
- [26] J. Timmer, C. Gantert, G. Deuschl, and J. Honerkamp, *Biol. Cybern.* **70**, 75 (1993).
- [27] M. van der Heyden, C. Diks, J. Pijn, and D. Velis, *Phys. Lett. A* **216**, 283 (1996).
- [28] H. Voss and J. Kurths, *Phys. Rev. E* **58**, 1155 (1998).
- [29] H. Abarbanel, *Analysis of Observed Chaotic Data* (Springer, Berlin, 1996).
- [30] H. Kantz and T. Schreiber, *Nonlinear Time Series Analysis* (Cambridge University Press, Cambridge, 1997).
- [31] P. Grassberger and I. Procaccia, *Physica D* **9**, 189 (1983).
- [32] A. Wolf, J. Swift, H. Swinney, and L. Vastano, *Physica D* **16**, 285 (1985).
- [33] G. Sugihara and R. May, *Nature* **344**, 734 (1990).
- [34] S. Elgar, R. Guza, and R. Seymour, *J. Geophys. Res.* **89**, 3623 (1984).
- [35] P. Grassberger, *Nature* **323**, 609 (1986).
- [36] J. Kurths and H. Herzel, *Physica D* **25**, 165 (1987).
- [37] D. Kaplan and C. Cohen, *Circulation Research* **67**, 886 (1990).
- [38] M. Kennel and S. Isabelle, *Phys. Rev. A* **46**, 3111 (1992).
- [39] A. Provenzale, R. Vio, and S. Cristiani, *Astrophys. J.* **428**, 591 (1994).
- [40] H. Voss, J. Kurths, and U. Schwarz, *J. Geoph. Res.—Space Physics* **101**, 15,637 (1996).
- [41] K. Leighly and P. O’Brien, *Astrophys. J.* **481**, L15 (1997).
- [42] J. Kurths *et al.*, in *Proceedings of the International School of Physics “Enrico Fermi”*, edited by G. C. Castagnoli (IOS Press, Amsterdam, 1997).
- [43] L. Smith, in *Mixing and Transport in the Environment*, edited by K. Beven, P. Chatwin, and J. Millbank (John Wiley & Sons, New York, 1994).
- [44] G. Zöller, R. Engbert, S. Hainzl, and J. Kurths, *Chaos, Solitons and Fractals* **9**, 1429 (1998).
- [45] S. Schiff and T. Chang, *Biol. Cybern.* **67**, 387 (1992).
- [46] T. Chang *et al.*, *Biophys. J.* **67**, 671 (1994).
- [47] S. Schiff *et al.*, *Biophys. J.* **67**, 684 (1994).
- [48] T. Schreiber, *Phys. Rev. Lett.* **80**, 2105 (1998).
- [49] P. Rapp, A. Albano, I. Zimmerman, and M. Mimenez-Montana, *Phys. Lett. A* **192**, 27 (1994).
- [50] J. Norris and T. Matilsky, *Astrophys. J.* **346**, 912 (1989).
- [51] H. Letho, B. Czerny, and I. McHardy, *Mon. Not. R. Astron. Soc.* **261**, 125 (1993).
- [52] L. Sachs, *Applied Statistics* (Springer, New York, 1984).
- [53] R. Miller and D. Siegmund, *Biometrics* **38**, 1011 (1982).
- [54] B. Lausen and M. Schumacher, *Biometrics* **48**, 73 (1992).
- [55] R. Dahlhaus, in *Robust and Nonlinear Time Series Analysis*, Vol. 26 of *Lecture Notes on Statistics*, edited by J. F. et al. (Springer, Heidelberg, 1984), pp. 50–67.
- [56] M. König, R. Staubert, and J. Wilms, *Astron. Astrophys.* **326**, L25 (1997).
- [57] M. König, S. Friedrich, R. Staubert, and J. Timmer, *Astron. Astrophys.* **322**, 747 (1997).
- [58] H. Negoro, S. Miyamoto, and S. Kitamoto, *Astrophys. J.* **423**, L127 (1994).
- [59] E. Liang and P. Nolan, *Space Science Rev.* **38**, 353 (1984).
- [60] J. Wilms, J. Dove, M. Nowak, and B. Vaughan, in *Proc. 4th Compton Symposium*, edited by C. Dermer, M. Strickman, and J. Kurfess (AIP, Woodbury, 1997), Vol. 410, p. 849.
- [61] D. Kaplan and L. Glass, *Understanding Nonlinear Dynamics* (Springer, New York, 1995).
- [62] W. Barnett *et al.*, *J. Econometrics* **77**, 297 (1997).
- [63] M. Aschwanden *et al.*, *Astrophys. J.* **505**, 941 (1998).
- [64] J. Timmer, *Phys. Rev. E* **58**, 5153 (1998).

FIGURE CAPTIONS

Fig. 1 A 3 s segment of the intermediate state time series.

Fig. 2 Analysis of a simulated shot noise process. (a) Segment of a realization of an exponential shot noise process with intensity $\rho = 0.1$ and decay time $\tau = 15$ sampling units. (b) The $Q(m)$ statistics, Eq. (14). (c) Significances $S(m)$, Eq. (13).

Fig. 3 Periodogram of the data (dots) and spectra (solid lines) calculated from the estimated parameters of the state space model of dimension one to three in log-linear scale (top) and log-log scale (bottom). Note that the spectra are virtually indistinguishable.

Fig. 4 Significances $S(m)$ of the $Q(m)$ statistics for lags up to 1000. (a) First segment of the intermediate state data set. (b–d) Results for the second to the fourth segment.

Fig. 5 Significances $S(m)$ analogous to Fig. 4. Dashed lines: Results for the raw data. Solid lines: Results for data after Kalman-filtering.

Fig. 6 Significances $S(m)$ of the $Q(m)$ statistics for lags up to 100. Dashed lines: Results for the raw data. Solid lines: Results for data after Kalman-filtering.

Fig. 7 Results from a simulation study using the fitted LSSM. The significances $S(m)$ of the $Q(m)$ statistics are calculated for the raw data (solid line) and the data after Kalman-filtering (dashed line).

Fig. 8 Significances $S(m)$ of the $Q(m)$ statistics and 2σ confidence regions calculated from the 32 segments of length 20,000 of intermediate state time series. Dashed line: Raw data. Solid line: Kalman-filtered data.

Fig. 9 Significances $S(m)$ of the $Q(m)$ statistics and twice the standard error calculated from the 19 segments of length 20,000 of the low state time series. Dashed line: Raw data. Solid line: Kalman-filtered data.

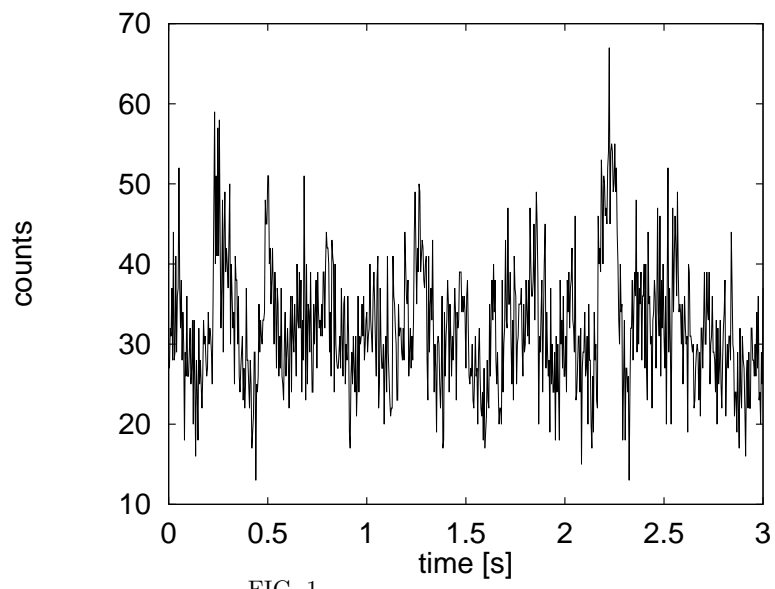


FIG. 1.

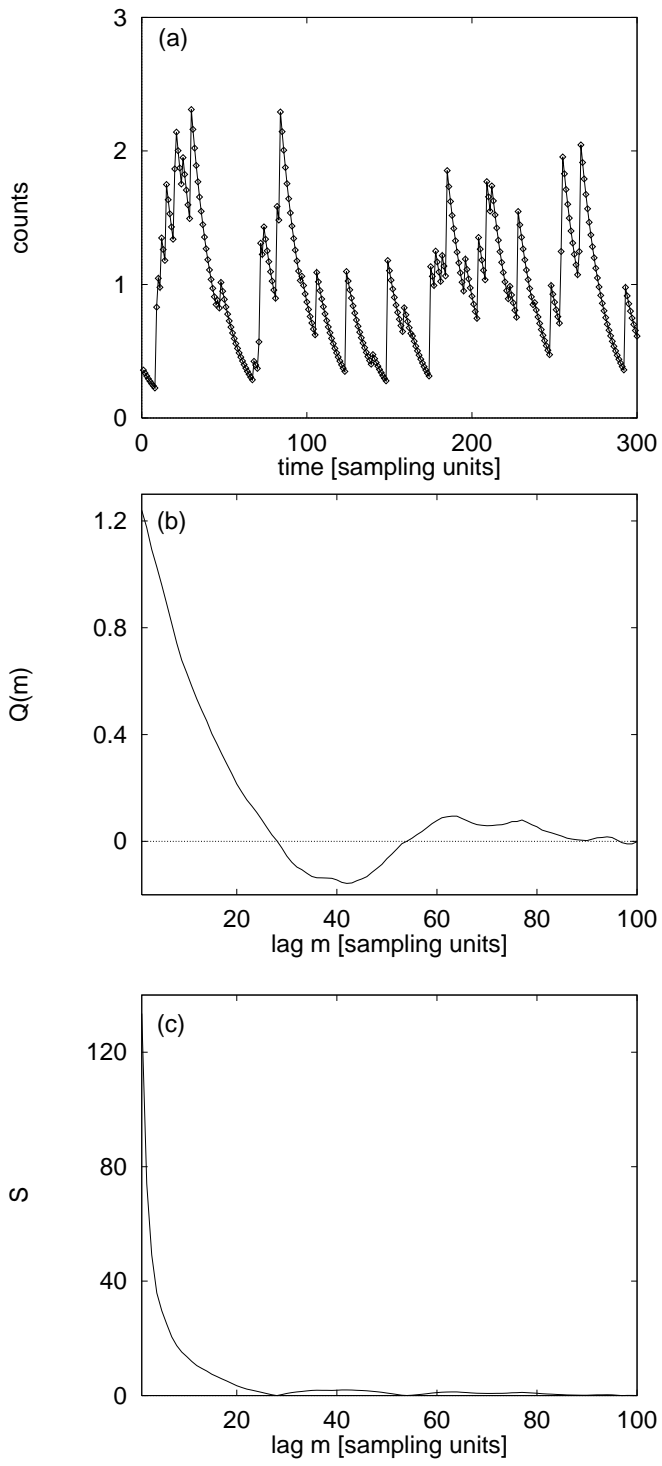
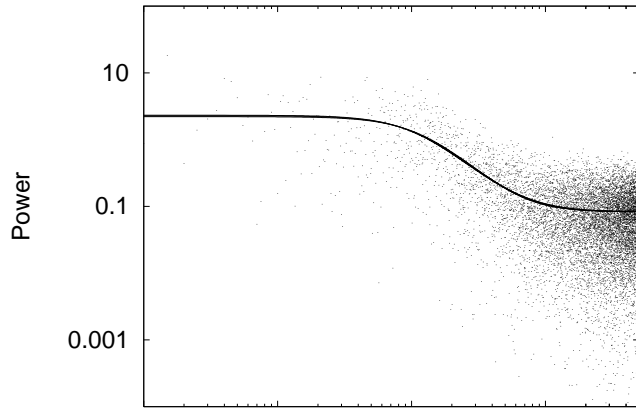
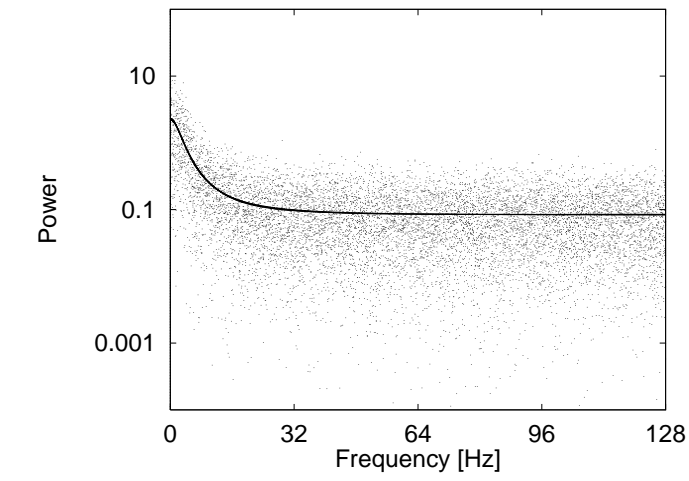


FIG. 2.



Frequency
FIG. 3.

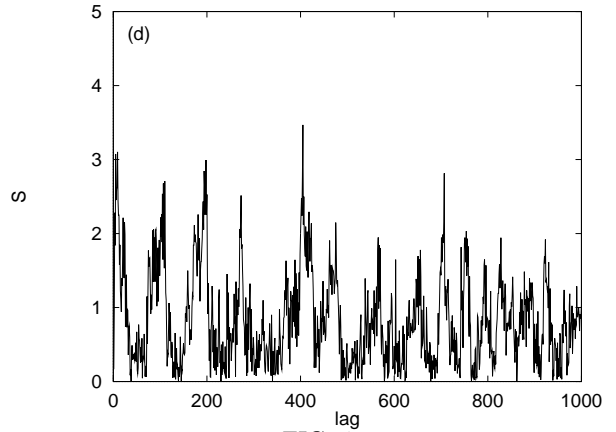
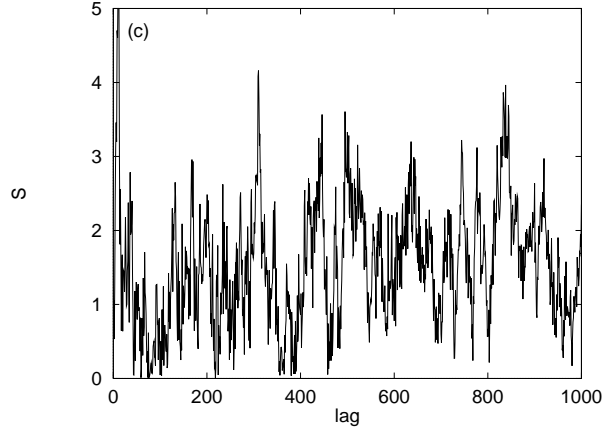
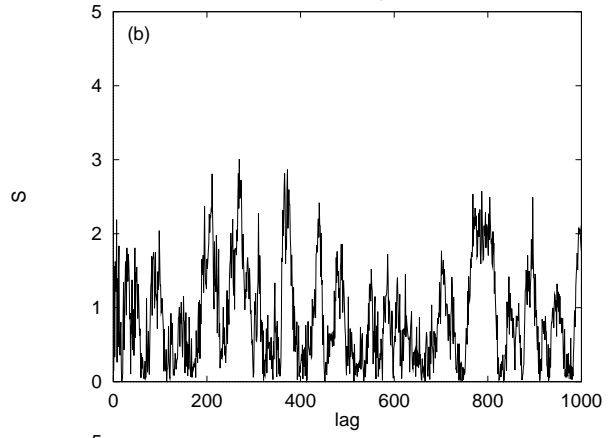
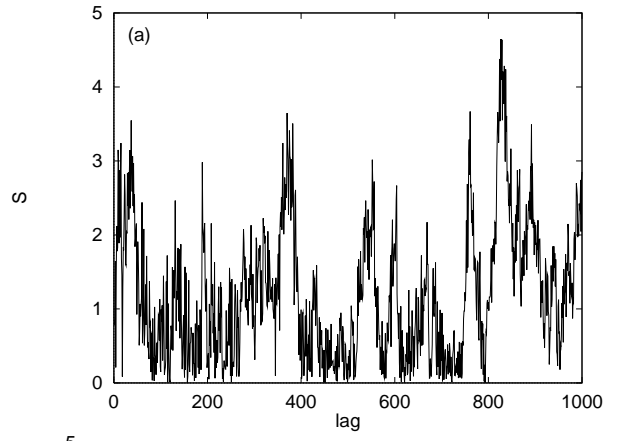
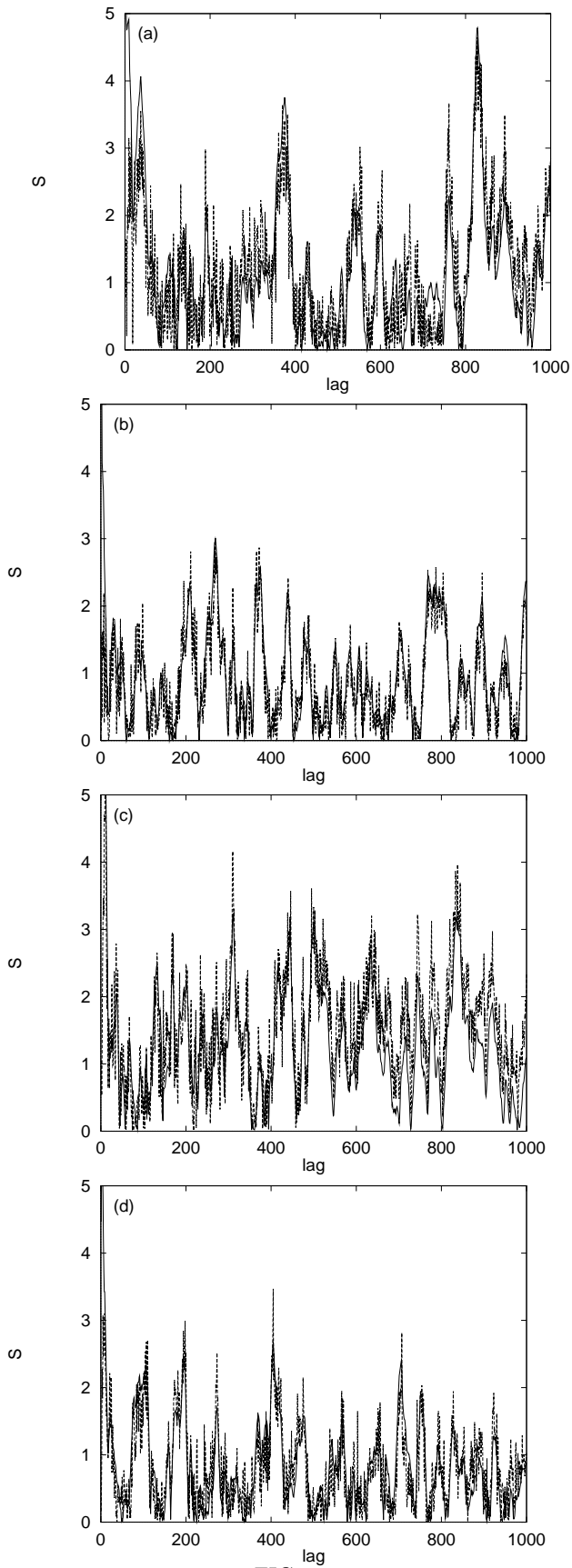


FIG. 4.



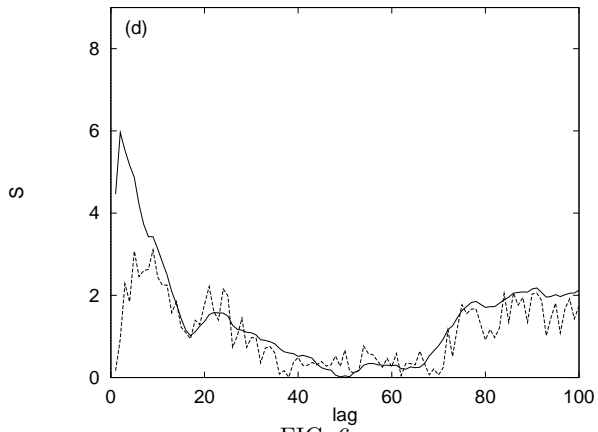
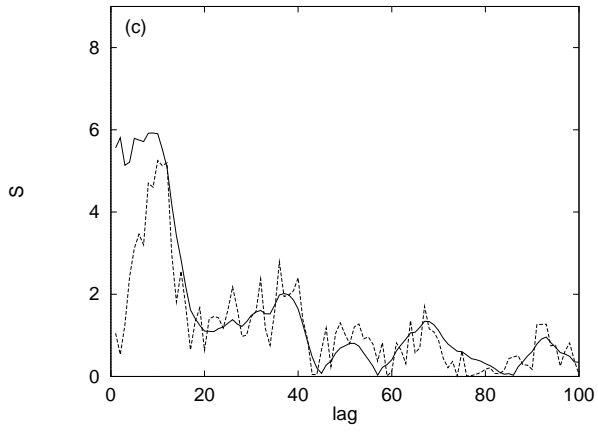
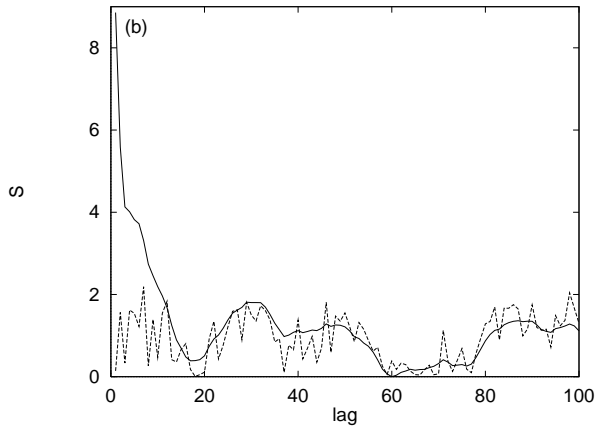
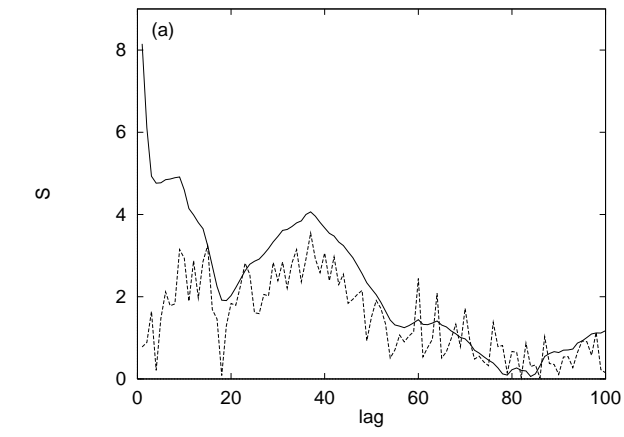


FIG. 6.

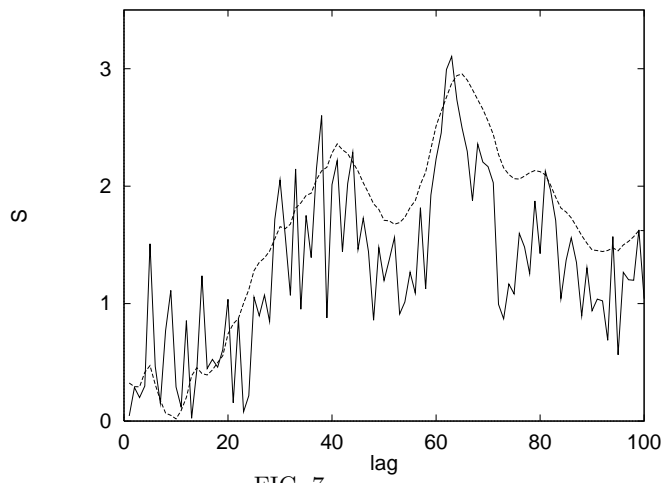


FIG. 7.

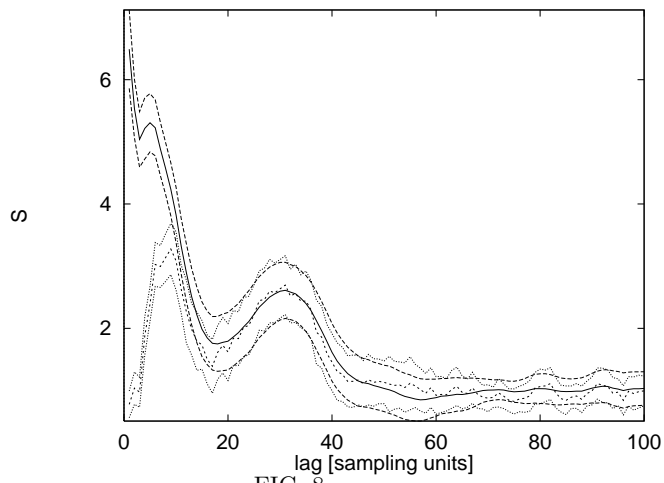


FIG. 8.

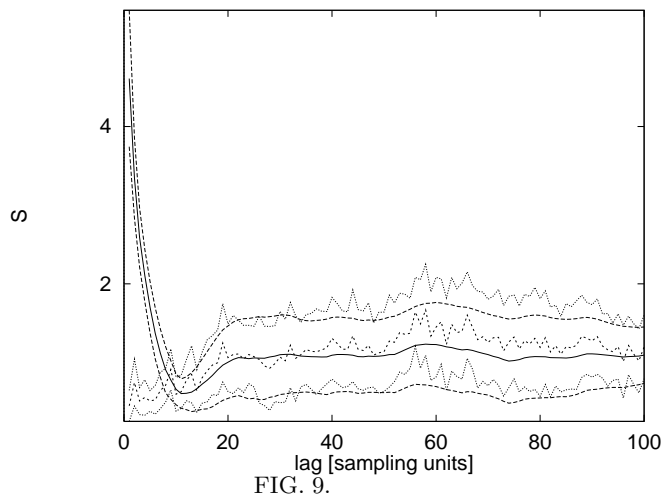


FIG. 9.